BIMA Optical Pointing Project. I.
The STV Video Camera

Jonathan Swift
UC Berkeley Radio Astronomy Lab
25 March 2002

ABSTRACT

This memo presents the first steps toward a functional optical pointing system at BIMA. The specifications of the STV video camera mounted on the optical pointing telescopes of the Hat Creek interferometer are shown. The sensitivity of the system has been empirically determined ($m_{zp} = 15.9^{\rm m}$) and simulations have shown that a signal to noise of ≈ 15 is needed to determine a centroid accurate to a $1''$ with 95% confidence. This means that a pointing solution can be obtained in a random field (stellar density averaged over the celestial sphere) with an integration time of a few seconds.

Introduction

The BIMA antennas could greatly benefit from quick and accurate pointing corrections. Having a feedback system that keeps the antennas pointed precisely on target will increase the sensitivity of the array while allowing for more consistent and accurate flux measurements. To achieve this with an optical guiding telescope, one needs a relatively sensitive CCD chip that can read out at a high rate. The STV, made by the Santa Barbara Instruments Group, is the latest in commercially available astronomical video cameras and offers both of these features.

The CCD is the TI TC-237 chip made by Texas Instruments and is a 656×480 pixel array sensitive to a range of wavelengths from $\sim$ 4000–10000 Å. The chip is cooled thermo-electrically to about 25° C below ambient with a quantum efficiency as a function of wavelength shown in Figure 1. Some other relevant specifications for the camera are shown in Table 1.

The camera can detect a $12^{\rm m}$ star at the 15σ level in about 1 s using the 10 cm pointing telescopes at BIMA. There is also the possibility of doing daytime pointing to a depth of $\sim 7^{\rm m}$ using an IR filter and possibly a polarizer. In this memo I briefly describe the STV camera and procedures and results of preliminary tests of the STV performance on the pointing optics at BIMA.

Specifications

The most basic numbers regarding the STV camera mounted on the pointing optics at BIMA are shown in Table 2. There are a few details and idiosyncrasies of this setup that are worth mentioning.

The STV comes with a control box and firmware which can perform such tasks as pointing error analysis and PSF fitting. However, this firmware is not flexible. I have had some success with

Table 1: Model TC-237 CCD Specifications

Pixel Array	656×480
Pixel Size	$7.4 \times 7.4\,\mu$m
Full Well Capacity	$20{,}000\,e^-$
Dark Current	$5\,e^-$/pixel/sec at 0°C
A/D Converter	12 bits
A/D Gain (max.)	$4.0\,e^-$/ADU (variable)
Read Noise (Typical)	$17\,e^-$ RMS

getting SBIG software engineers to update the firmware, but it is a long process with the benefits not convincingly outweighing the effort.

The STV control box can be run from a PC using Windows software available free from the SBIG website [3]. The PC connection is established via an RS-232 cable which is sufficient for issuing commands but slow for image transfer taking up to 30 s to download a single image. There is also a "video out" port which takes a standard coaxial cable with an RCA connector.

The field of view is variable depending on whether pixels are binned or read out individually. If you want to read out every pixel individually, the STV will automatically read out the central

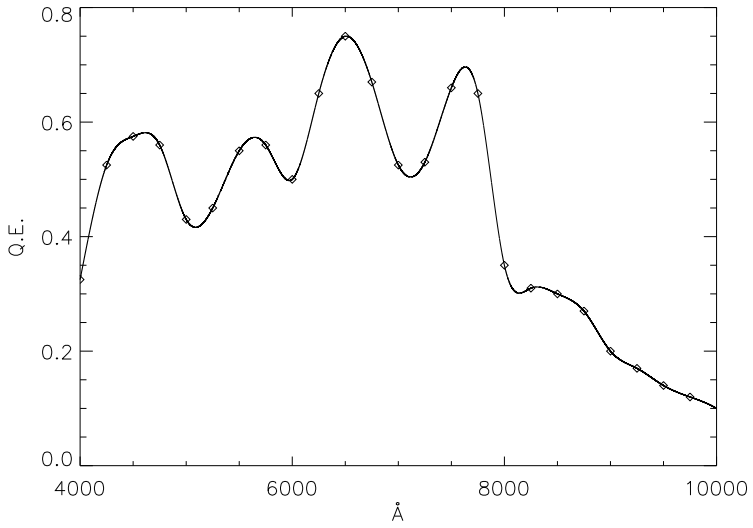

Figure 1: Quantum efficiency of the TC-237 CCD chip as a function of wavelength. A cubic spline interpolation has been performed between data points.

320×200 pixels of the chip giving a field of view of $9'.1 \times 5'.6$ with a $1''.7$/pixel image resolution. It is also possible to bin pixels 2×2 or 3×3 giving field sizes of $18'.1 \times 11'.3$ and $18'.6 \times 13'.6$ respectively. The STV operates this way because there is a limit to the overall number of bytes an image can consume.

The 10 cm lenses on the BIMA optics are significantly chromatic. This may be a primary concern if any kind of filter is going to be used. When the 850 μm IR filter was implemented without compensating for the chromaticity of the lens by refocusing, we found that the PSF was broadened by a factor of 2.

Table 2: Telescope Specifications

Parameter	Pointing Telescopes (BIMA)
Type	Refractor
Primary Diameter	10 cm
Focal Length	90.0 cm
Plate Scale	$1''.7$/pixel
Field of View with STV	$18'.6 \times 13'.6$ (max.)

Relevant Equations

The standard way to achieve a final image of the sky using a CCD array is to subtract the dark current and then normalize pixel to pixel variations by dividing by a sky, or flat, frame. The flat and dark frames must be well calibrated to avoid injecting noise into the final image. This requires taking many flats and darks which is not practical for what we want to do so I will assume that our raw image is our final frame. This makes the signal to noise calculation much more straightforward. Assuming that all signals follow Poisson statistics, the relevant noise sources are then

(1) Readout noise = R

(2) Photon noise on the source signal (S) = $\sqrt{S}$

(3) Photon noise on the background signal (B) = $\sqrt{B}$

(4) Noise on the dark current signal (D) = $\sqrt{D}$

Here S, B, D, and R are given in electrons per second and can be derived from the observed counts in A/D Units (ADU) by multiplying by the gain g given in e^-/ADU. Random, independent noise sources can be added in quadrature, therefore the signal to noise ratio (SNR) for an image of

integration time t is given by

$$\mathrm{SNR} = S\sqrt{t}\cdot\left[S+\sum_{i=1}^{n}\left(B+D+\frac{R^2}{t}\right)\right]^{-1/2}. \tag{1}$$

Here S is the total signal summed over all pixels and the sum accounts for the fact that B, D and R can vary from pixel to pixel. The square root of t in the numerator comes from the fact that signal counts increase linearly with time while noise increases as $\sqrt{t}$. The division by t in the read noise term is needed since read noise is constant with respect to integration time. We will be concerned solely with stars (points), so we can estimate the number of pixels in which signal lies, n, from the seeing conditions and the plate scale. If a stellar object has a seeing disk of diameter θ_S while each CCD pixel is θ_{CCD} on a side, then the number of pixels covered by the star's image is approximately

$$n = \frac{\pi}{4}\left(\frac{\theta_S}{\theta_{CCD}}\right)^2. \tag{2}$$

The photo-electron detection rate from flux collected by a telescope with an effective aperture of area A_{eff} from a source of apparent magnitude m transmitted by an optical system of efficiency $\tau(\lambda)$ onto a CCD with quantum efficiency $\eta(\lambda)$ is

$$S = (hc)^{-1}\int_{\lambda_{low}}^{\lambda_{high}}\tau(\lambda)\,\eta(\lambda)\,A_{eff}\,F_\lambda(0)\cdot 10^{-0.4m}\,\lambda\,\mathrm{d}\lambda \quad \text{electrons s}^{-1} \tag{3}$$

where $F_\lambda(0)$ is the flux from a zeroth magnitude standard star above the atmosphere (see *e.g.* [1] pg. 387 or [2] pg. 304 for flux calibration). Dividing (3) by the gain g in units of e^-/ADU gives the total number of counts. Setting the number of counts per second equal to unity, we derive the "zeropoint" magnitude m_{zp} of the instrument.

$$m_{zp} = 2.5\log_{10}\left[(h\,c\,g)^{-1}\int_{\lambda_{low}}^{\lambda_{high}}\tau(\lambda)\,\eta(\lambda)\,A_{eff}\,F_\lambda(0)\,\lambda\,\mathrm{d}\lambda\right]. \tag{4}$$

The quantity m_{zp} is the apparent magnitude of an A0 star that will produce one count per second in the instrument above the Earth's atmosphere, and is a conversion factor between number of source counts per second and apparent source magnitude. The zeropoint can be obtained empirically by observing a standard star and plotting the quantity $m_{std} + 2.5\log_{10}[S\,(\mathrm{ADU/s})]$ as a function of airmass and extrapolating to zero airmass.

Knowing m_{zp} then allows for a limiting magnitude calculation given an integration time and desired SNR. In the limit that the noise term is dominated by the readout noise, we can invert (1) and solve for source counts per second in terms of SNR. Using the definition of the zeropoint magnitude we have

$$\mathrm{m}_{lim} = m_{zp} - 2.5\,\log_{10}\left(\mathrm{SNR}\cdot\frac{R\sqrt{n}}{t\cdot g}\right). \tag{5}$$

Observations and Results

The first observations with the STV camera mounted on the BIMA optics took place on 17 May 2001 and were aimed at empirically determining the sensitivity of the camera. Preliminary images were taken of standard star fields and compared to finding charts. An example of a typical image can be seen in Fig. 2.

Standard stars were observed over a range of elevations and a zeropoint was determined using the procedure outlined in the previous section. The data and extrapolation can be seen in Fig. 3.

To get a feel for how much signal to noise is needed to obtain a reliable centroid, simulations were run which generated varying amounts of signal on top of gaussian noise. A 2-D gaussian fit was then performed using the IDL task `GAUSS2DFIT`. It was determined that a total signal to noise [as defined in (1)] of 10 produced a centroid solution accurate to $1''$ with 50% confidence. Simulated $15\,\sigma$ detections produced acceptable centroid solutions with 95% confidence. A grey scale depiction of the signal to noise ratio is shown in Fig. 4.

Given the zeropoint and the necessary signal to noise we can calculate what integration times are needed to see a star of a particular magnitude. Another relevant quantity is the number of stars that can be expected to be above the noise limit for a given integration time in a random field. We cannot determine these statistics empirically with our limited number of images. However we have used the numbers from [1] and find good agreement with our data. The results of these calculations are summarized in Table 3.

Some daytime tests were performed at BIMA with limited success. The problems we encountered

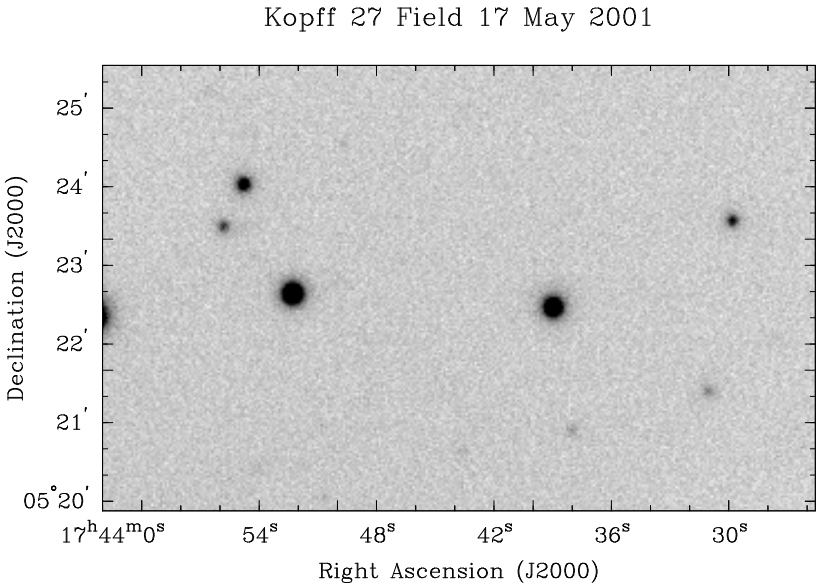

Figure 2: This is a dark subtracted 60s exposure toward the field of standard star Kopff 27. The magnitude limit of this image is $\sim 16^{\rm m}$.

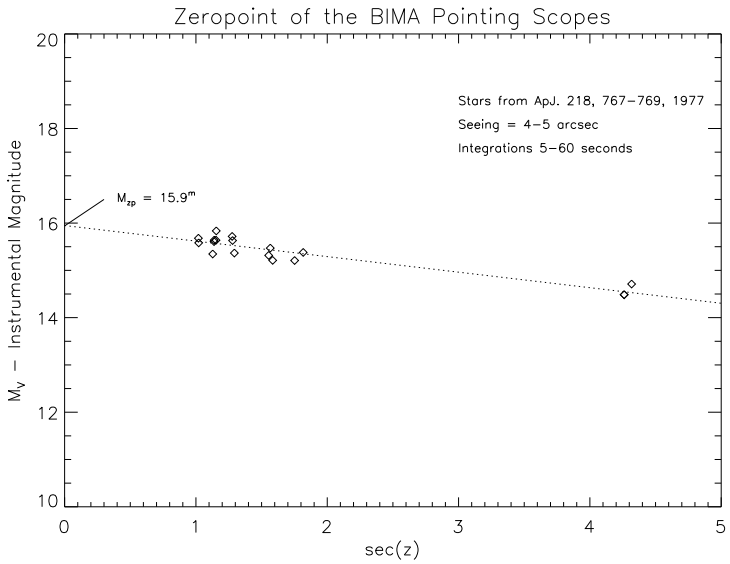

Figure 3: The quantity $m_{std} + 2.5\log_{10}(S)$ as a function of airmass. Extrapolation to zero airmass gives the zeropoint magnitude of the instrument.

M_V	Integration Time	Stars per Field
5	0.001	0.0004
6	0.004	0.004
7	0.01	0.004
8	0.03	0.01
9	0.06	0.03
10	0.16	0.09
11	0.40	0.24
12	1.0	0.4
13	2.5	1.1
14	6.3	3
15	16	6
16	40	12
17	100	24
18	250	48

Table 3: 15σ sensitivity of the BIMA 10cm pointing telescope with a plate scale of 1.7 arcsec/pixel and 4.5 arcsecond seeing.

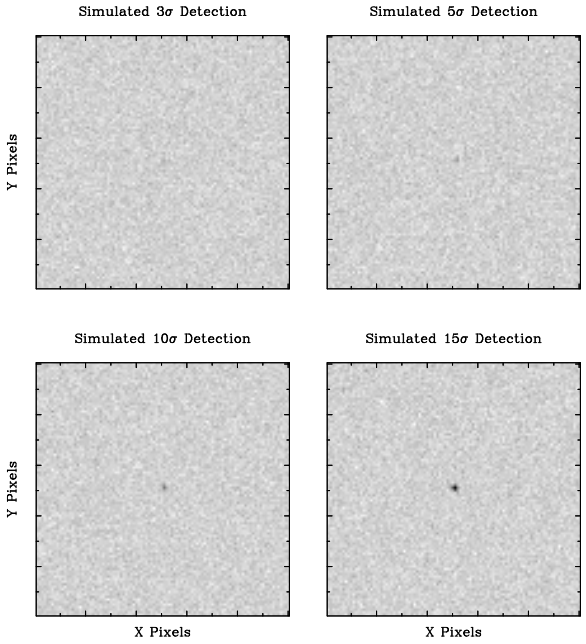

Figure 4: These simulations have shown that the threshold for a reliable centroid determination is 10σ. In all images, the "star" is located at the center of the image.

were of both the hardware and software variety. It was difficult to focus the camera because individual images were noisy and the brightest objects were extended (e.g. Venus). Experiments with IR filters and polarizers to eliminate Rayleigh scattered photons were promising but inconclusive given the quality and amount of data collected.

The brightness of the day sky (even with an IR filter) necessitates stacking images because of the CCD well sizes. This introduces a number of problems. The STV firmware will only stack 100 images allowing ~ 1 s of total integration time for the full 10 cm aperture with the 850 μm IR filter. Another problem is that stacking images compromises the flatness of the image. I'm not sure why this is, perhaps due to the fact that each pixel is near saturation in each stacked frame, but it is a noticeable effect. Lastly, each individual frame is only allowed 10 bits and the final image is allowed 15 bits which imposes hard limits on the individual frame integration time and total integration time, respectively. These facts about the STV are not easily changeable and are the limiting factor for daytime observations.

Despite daytime difficulties, our night time data clearly show that optical pointing is possible given commercially available technology.

Radio vs. Optical Collimation

Our next task is to characterize the optical and radio collimation to determine the accuracy of applying an optical solution to the radio poiniting tables. The structural response of the antennas will create an error between the optical and radio pointing as a function of elevation. The aluminium pointing scope mounts are bolted to the steel structure of the telescope and so collimation errors will also be a function of temperature (time) due to the differing coefficients of linear expansion for the two materials. It will be possible to characterize and decouple these two effects by making simultaneous radio and optical observations over a range of elevations and temperatures.

We have chosen a list of SiO maser stars for this experiment which provide plenty of optical and radio signal to obtain pointing solutions in both wavelength regimes (see Fig. 5). We will

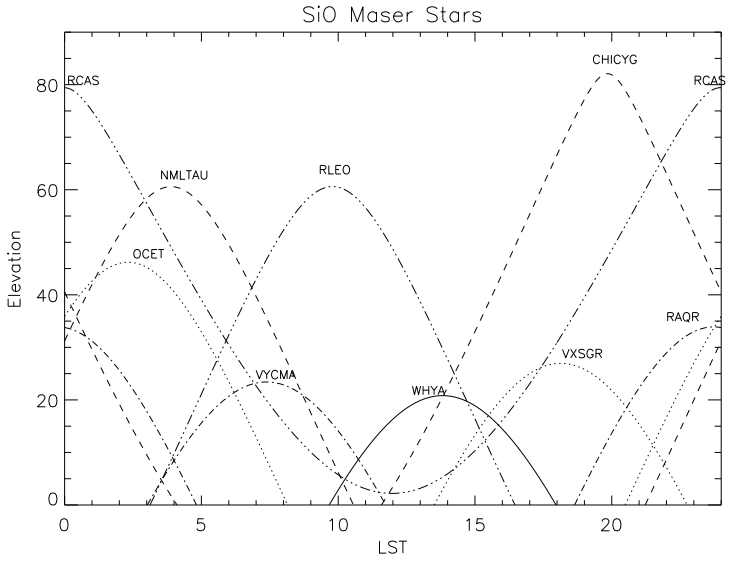

Figure 5: Elevations of the 9 SiO maser stars as a function of LST.

perform a 10 pointing cross with the interferometer in a narrow band correlator window centered on SiO $(2 \rightarrow 1)$, $v = 1$ while leaving the STV shutter open. This will give us a cross of star images on the CCD and baseline amplitudes which can be fit with a 2-D gaussian. Since the sources of radio and optical emission are coincident (to within $\sim$ 30 mas) it is an ideal comparison. Simultaneous pointing solutions for a range of elevations over the course of a night will allow us to characterize the stability and predictablility of the optical and radio collimation.

References

[1] Allen's Astrophysical Quantities, 4th edition, ed. Cox, Arthur N., AIP Press, New York, 2000.

[2] McClean, Ian S., Electronic Imaging in Astronomy, John Wiley and Sons, Chichester, England, 1997.

[3] `www.sbig.com`